CellPress
OPEN ACCESS

Supplemental figures

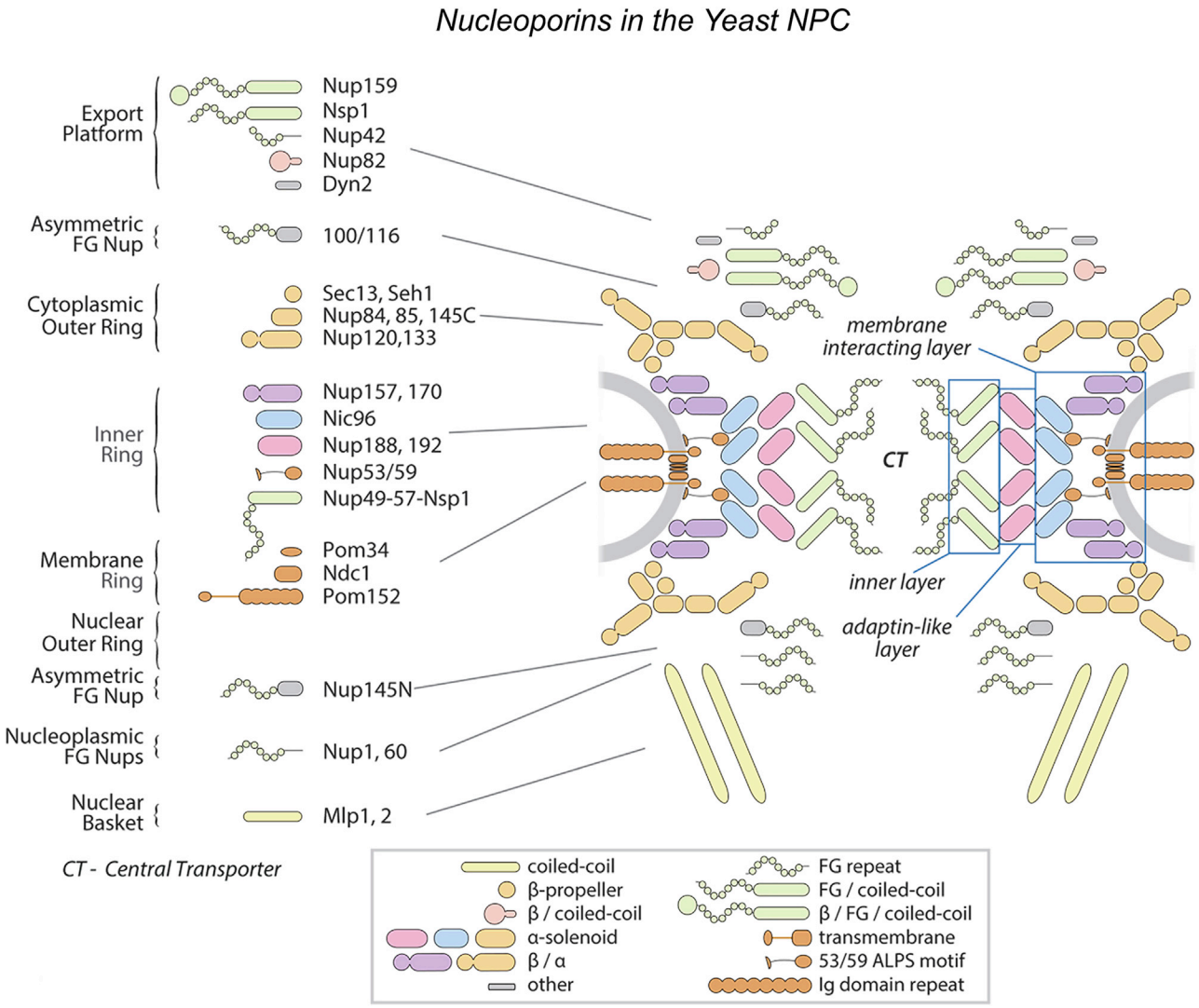

Figure S1. Nucleoporins within the yeast NPC, related to Figures 1, 2, 3, 4, 5, 6, and 7

Nups in the core scaffold are arranged into distinct rings: radial layers within a spoke are indicated within light blue boxes on the right.

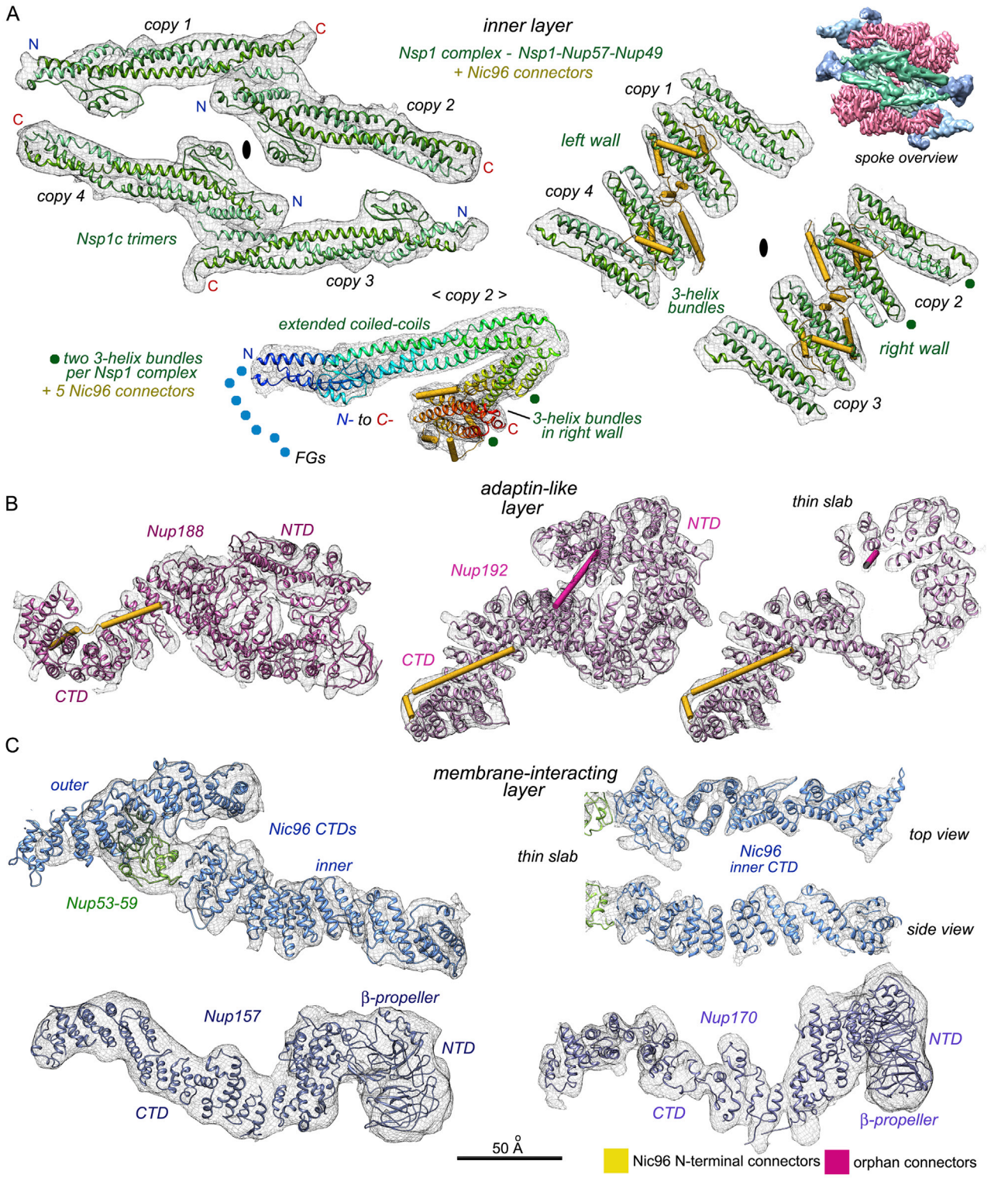

Figure S2. Local fit of Nups within the 3D map of the isolated spoke. An icon view shows the color coding for three layers in the spoke, related to Figures 1, 2, and 3

A. (**left**) Four Nsp1 complex trimers in the inner layer contain extended coiled coils that face into the central channel. Individual copies are indicated (copy 1-4, N- to C-) along with the local 2-fold axis (black ellipse). (**right**) diagonal walls formed by 3-helix bundles with bound Nic96 connectors. (**lower**) The N- to

(legend continued on next page)

C- connectivity for helices in copy 2 is shown in rainbow coloring. FG domains at the N terminus are indicated by blue dots along with 3-helix bundles and Nic96 connectors.

B. Nups from the adaptin-like layer: (**left**) Nup188 with Nic96 connector helices. (**right**) Nup192 with helical connectors (in gold and pink) with a thin slab view on the far right.

C. Nups from the membrane interacting layer: (**top left**) a pair of Nic96 CTDs with a bridging Nup53-Nup59 pair; (**top right**) two views of the inner copy of Nic96 at a higher threshold. (**bottom**) paralogs Nup157 and Nup170. Scale bar is indicated for all model panels.

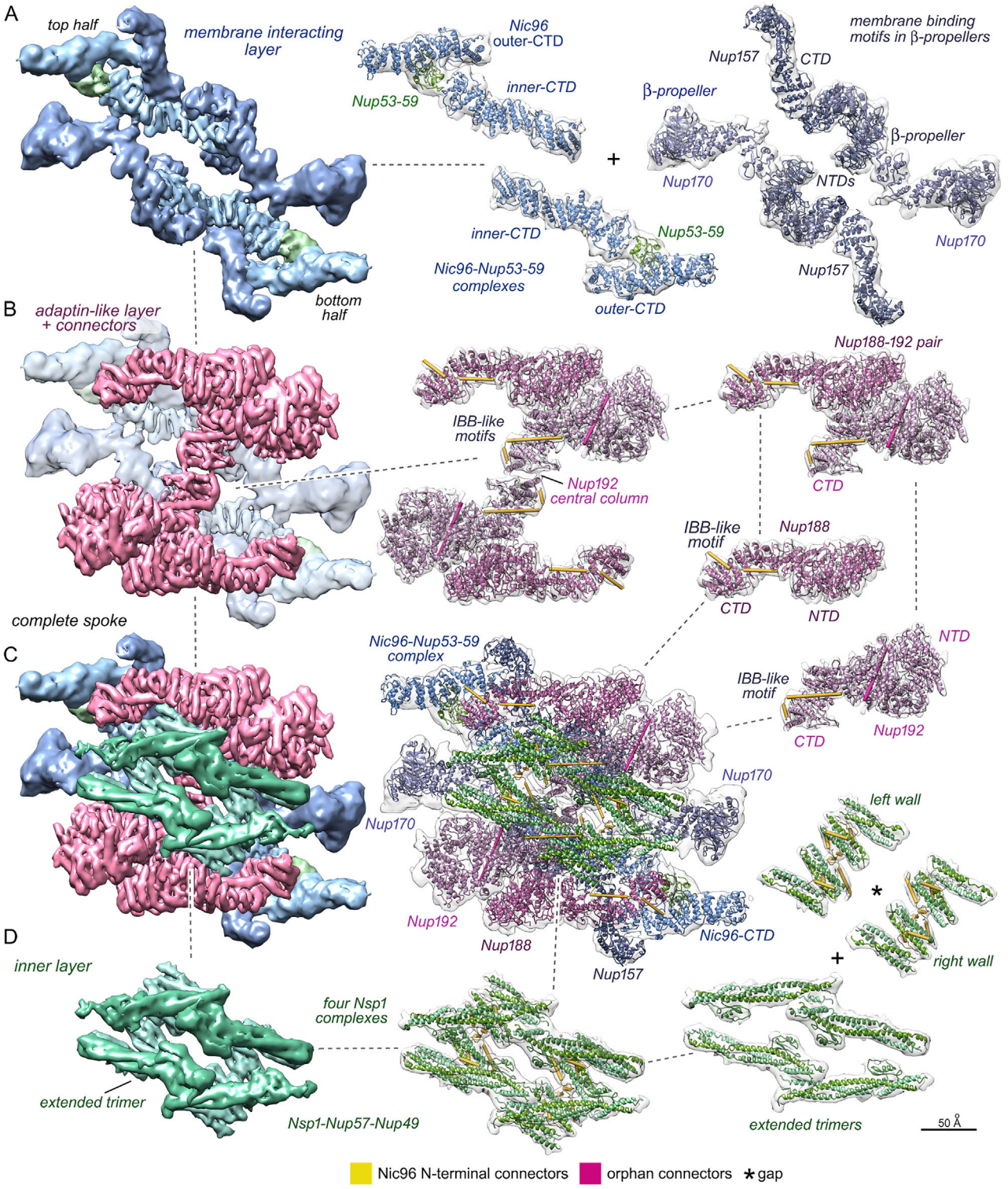

Figure S3. Functional division of the spoke at sub-nm resolution, related to Figures 1, 2, and 3

A. (**left**) The membrane interacting layer is shown as an isosurface. (**center**) 2-fold related Nic96 CTD pairs linked by Nup53-Nup59 heterodimers. (**right**) Two diagonal Nup157-Nup170 pairs.

B. (**left**) The central adaptin-like layer contains two Nup188-Nup192 pairs with bound connector helices. (**middle**) Nup192 CTDs form a central column that encompasses two IBB-like motifs. (**right**) Exploded view of the adaptin layer and its fit within the spoke indicated with dashed lines.

(legend continued on next page)

C. (**left**) A complete spoke with three major layers. (**center**) Docked Nups displayed as ribbons within the spoke.
D. (**left**) The inner layer contains two pairs of laterally offset Nsp1 complexes related by two-fold symmetry. (**middle** and **right**) Nsp1 complexes and connector rods are docked into transparent 3D maps of the inner layer that has been sub-divided into extended trimers which face into the central channel and two diagonal walls formed by 3-helix bundles. All panels are on the same scale, as indicated.

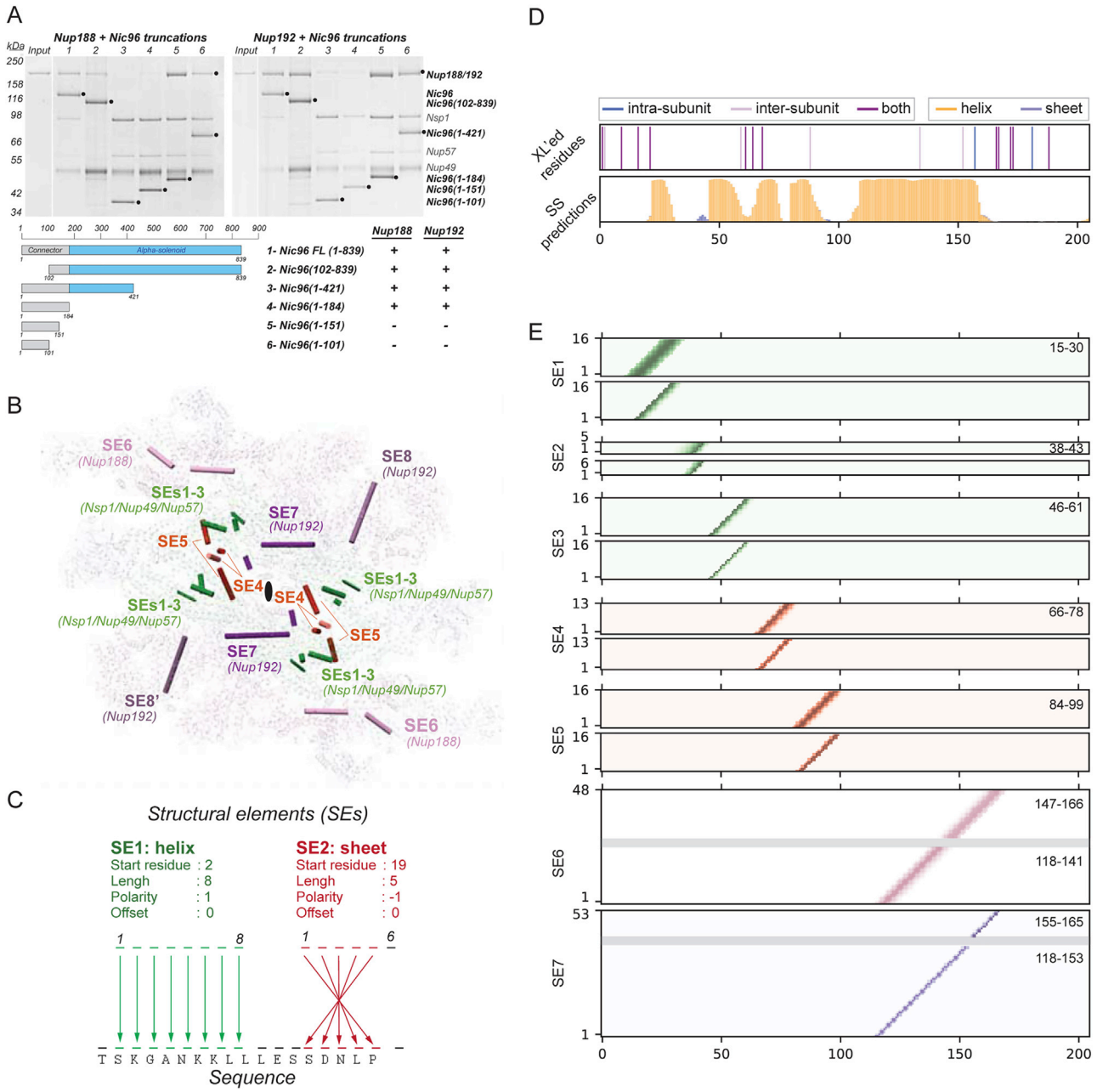

Figure S4. Integrative threading of orphan structure elements, related to Figure 3

A. Nup188 and Nup192 interact within an overlapping region of the Nic96 flexible connector. (**Top**) SDS-PAGE gels with results of *in vitro* reconstitution experiments between Nup188 (**left**) or Nup192 (**right**) with different Nic96 truncation mutants. Relevant proteins are indicated with a dot and their identity is indicated on the right. (**Bottom**) Schematic showing the boundaries of the Nic96 constructs (**left**) and a summary of the *in vitro* reconstitution results (**right**). FL, full length.

B. SEs in a spoke are indicated and elements 6 and 7 include two orphans. The SEs are grouped into five groups based on symmetry: 1) SEs 1-3 bind to the Nsp1/Nup49/Nup57 coiled-coils (green), 2) SEs 4 and 5 localize between coiled-coils (red) at the interface between half walls, 3) SE 6 binds to the Nup188 CTD (pink), 4) SE 7 binds to the Nup192 CTD (dark purple), and 5) SE 8 and 8' bind to the Nup192 NTDs (light purple).

C. Application of SE movers for integrative threading. The specification of an SE includes a secondary structure designation, a set of Cα coordinates, and four keys that map these coordinates to residues in the primary sequence.

D. Relevant cross-links and secondary structure predictions used for integrative threading of the Nic96 NTD.

E. Residue occupancy of good-scoring models after enumeration of all possible states. Each bin represents the mapping of a residue in sequence (x axis) to a coordinate in a structure element (y axis). Darker colors indicate that 100% of the good-scoring models map the corresponding residue to this structure element coordinate. Gray regions indicated helices that are bent or have missing segments.

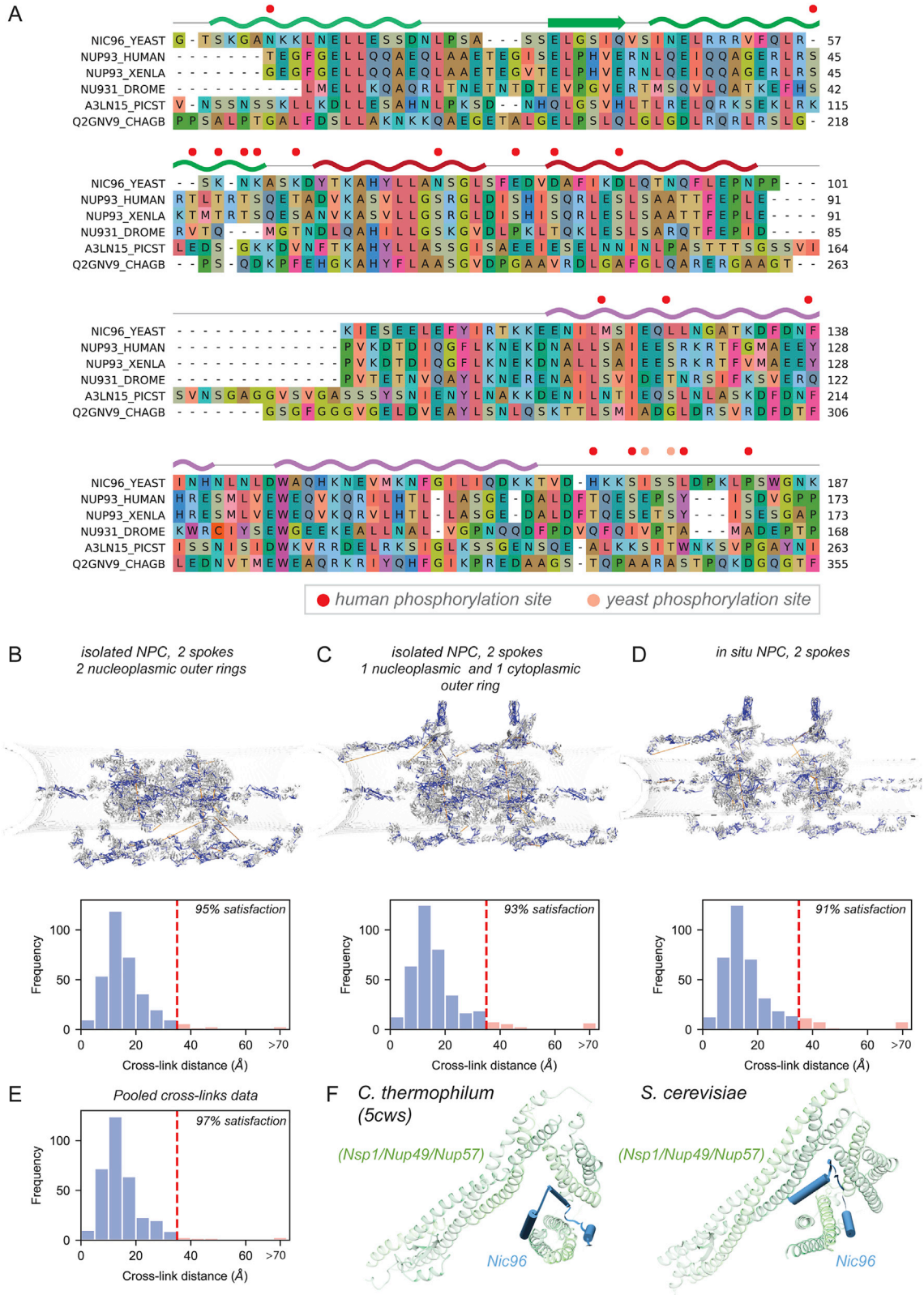

(legend on next page)

Figure S5. Validation of spoke orphans and NPC models, related to Figures 1, 2, 3, and 4

A. Sequence alignment for Nic96 NTD orthologs: *S. cerevisiae* (yeast), *Homo sapiens* (human), *Xenopus laevis* (xenla), *Drosophila melanogaster* (drome), *Pichia stipitis* (picst), and *Chaetomium globosum* (chagb). The secondary structure of the SE centroid assignments is shown above the sequence alignment. Mapped phosphorylation sites from human and yeast are shown as red and pink dots, respectively.

B. Satisfaction of unique chemical cross-links for the isolated NPC. Chemical cross-links were mapped onto the structure of adjacent spokes. Satisfied cross-links with Cα–Cα distances that fall below the 35 Å threshold are in blue. Violated cross-links with Cα–Cα distances larger than 35 Å in orange. The histogram shows the distribution of the cross-linked Cα–Cα distances.

C. Same as in panel B for a model of the isolated NPC created *in silico* with one nucleoplasmic and one cytoplasmic outer ring.

D. Same as in panel B for the *in situ* NPC model.

E. Cross-link satisfaction summed over all three models.

F. (**left**) Ribbon representation (light green) of the X-ray crystal structure of the *C. thermophilum* Nsp1/Nup49/Nup57 with the Nic96 R1 N-terminal SLiM. (**right**) Cryo-EM structure for this complex from *S. cerevisiae*. Nic96 connectors are shown as blue cylinders and strands.

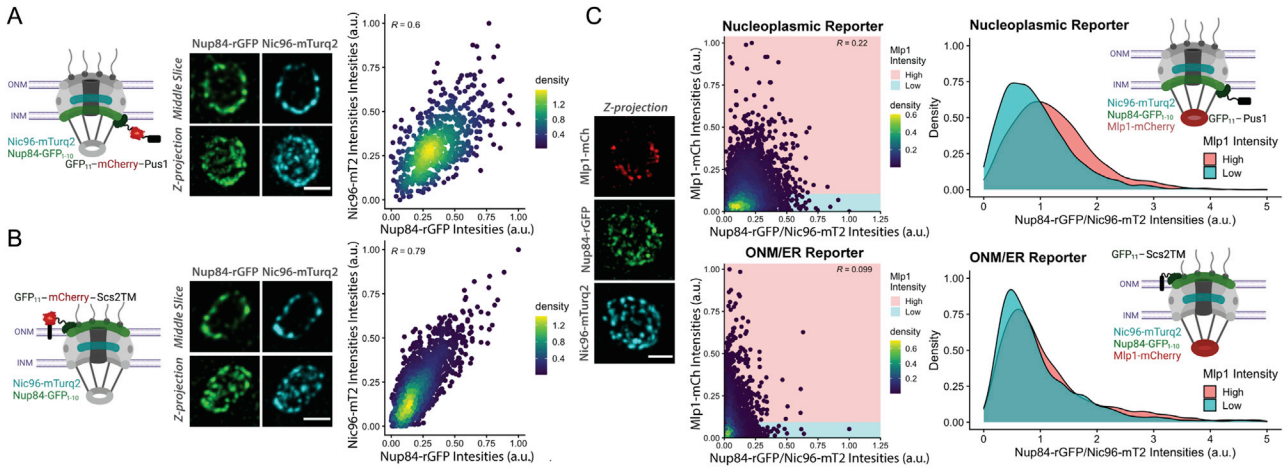

Figure S6. Quantitative fluorescence imaging of the double outer ring, related to Figure 4

A./B. (**left**) Schematic of the split-GFP system used to visualize outer ring complexes at the nucleoplasmic face of the NPC using a nuclear-localized GFP_{11}-mCherry-Pus1 reporter or at the cytoplasmic face using a GFP_{11}-mCherry-Scs2TM reporter localized to the outer nuclear membrane. Interaction of the GFP_{11} reporter with Nup84-GFP_{1-10} results in reconstitution of GFP (rGFP) and fluorescence; (**middle** and **right**), representative images and 2D density plots of Nup84-rGFP and Nic96-mTurq2 fluorescence intensities from strains expressing the nucleoplasmic (**panel A**) or the cytoplasmic (**panel B**) GFP_{11} reporter on the NE. Equivalent reconstitution of rGFP signal for both reporters shows that all NPCs have outer ring complexes on both their nuclear and cytoplasmic sides. A total of 662 (**panel A**) and 2720 NPCs (**panel B**) were analyzed. R, Pearson's correlation coefficient.

C. (**left**) A representative image of cells expressing Nup84-GFP_{1-10}, Nic96-mTurq2 and Mlp1-mCherry with a nucleoplasmic GFP_{11}-Pus1 reporter. (**middle** and **right**) Density plots showing the distribution of Nup84-rGFP intensities (normalized to Nic96-mTurq2 intensities) for NPCs with Mlp1 intensities greater than ("High") or below ("Low") the mean Mlp1 intensity value. Additional rGFP signal in the "High" Mlp1 NPCs for only the nuclear reporter shows that those NPCs have additional nuclear outer rings; moreover, NPCs in NE adjacent to nucleoli lack this extra outer ring signal, and are "Low" in Mlp1 intensity (**left panel**). A total of 4277 (nucleoplasmic reporter) and 4202 (ONM reporter) NPCs were analyzed. Schematics for panels F-H created with BioRender.

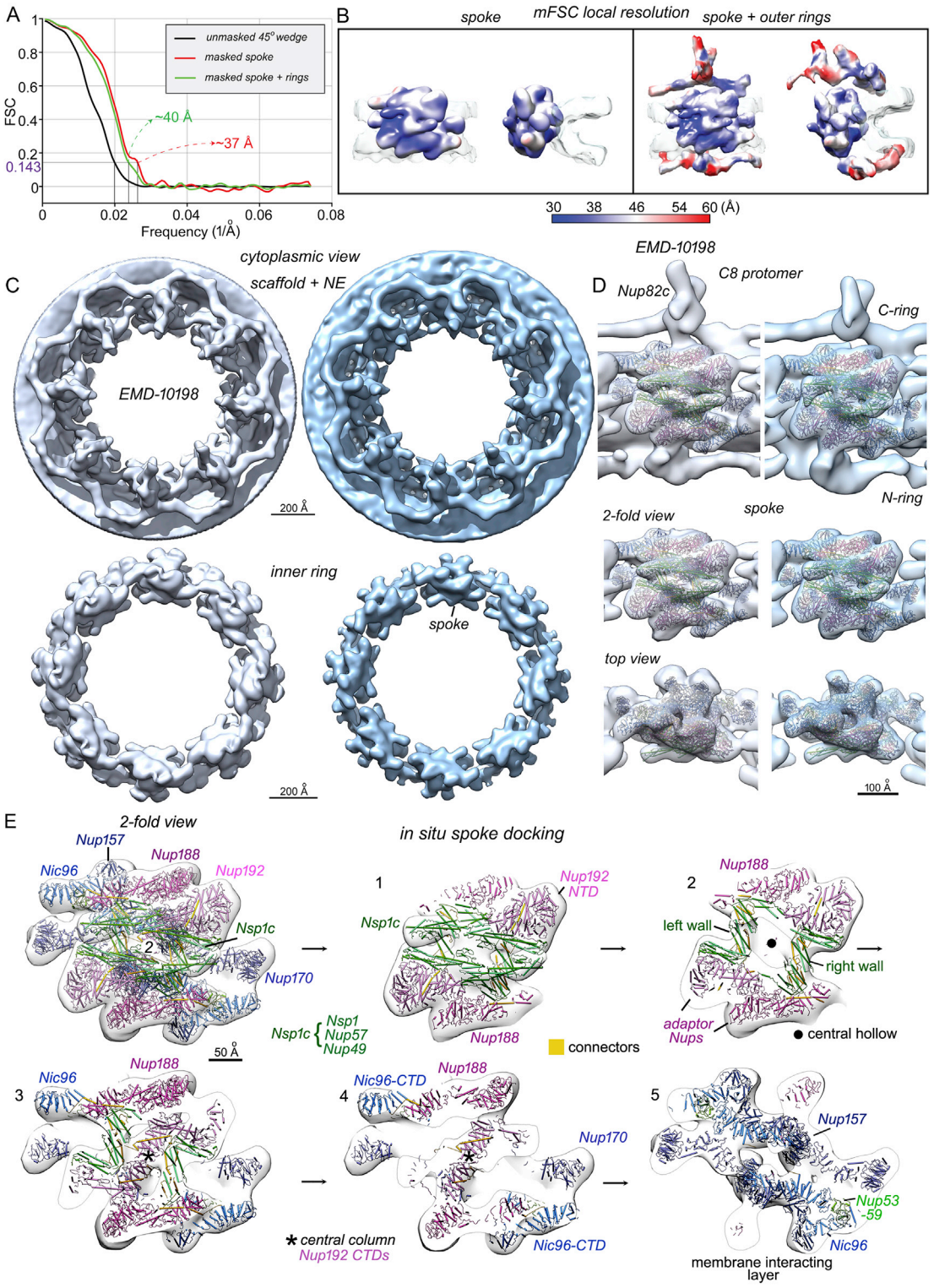

Figure S7. Resolution of the *in situ* NPC, comparison with a previously determined tomographic structure and molecular docking into the spoke, related to Figures 5 and 6

A. FSC curves for the spoke (red) and the full protomer (green) along with a comparison of unmasked half volumes (black).

B. Local resolution calculated with mFSC displayed on the 3D map for the spoke (**left**) and a full C8 protomer (**right**).

(legend continued on next page)

C. Side-by-side comparisons for 3D maps from EMD-10198 (Allegretti et al., 2020; in gray) and the current structure (in blue; EMD-24258) at a threshold that encloses the inner and outer rings. (**top**) Full 3D maps; (**bottom**) segmented inner rings.

D. Each column shows the density map for the C8 protomer and two views of the spoke with docked models. (**left**) EMD-10198, (**right**) current density map.

E. (**top left**) A front view of the *in situ* spoke with docked molecular models for the Nups: panels 1-5 show sequential cross-sections. The density map is sufficient to resolve two diagonal walls with a central hollow, a central column formed by Nup192 CTDs and to delineate larger Nups, shown as cylinders and strands. Scale bars are indicated on appropriate panels.

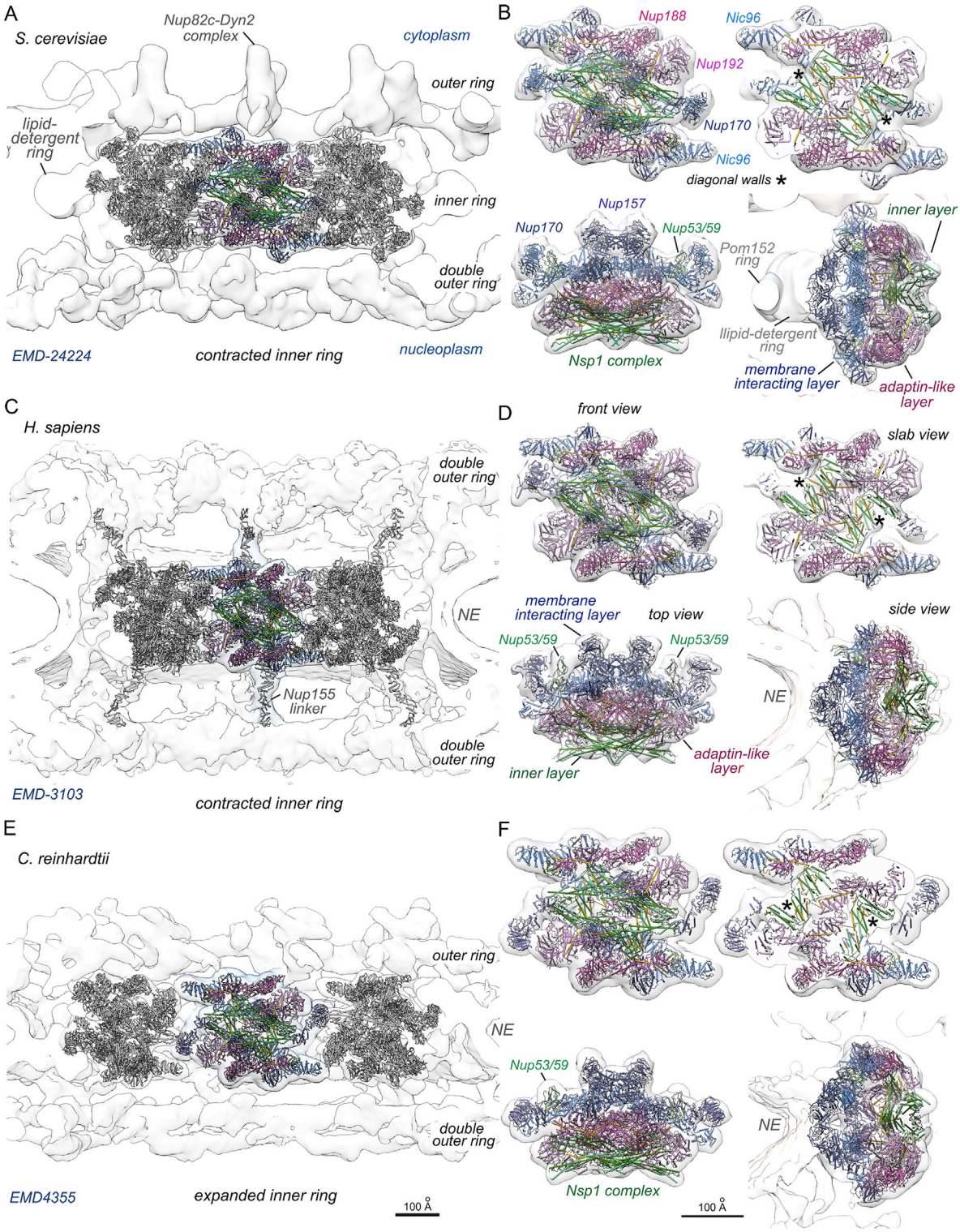

Figure S8. Structural conservation of the spoke and variable NPC architecture across species, related to Figures 1, 2, and 5

A. A central cross-section for three spokes within a composite map of the isolated, yeast NPC truncated to ~25Å resolution.

B. Four characteristic views of the isolated yeast spoke with the docked model. Individual Nups are labeled and the two diagonal walls are indicated with asterisks. The Pom152 ring and lipid-detergent ring are shown in the side view.

(legend continued on next page)

C. A central cross-section of the human NPC with a contracted inner ring (EMD-3103; (von Appen et al., 2015)). Human Nup155 linkers (in gray) were included in the computational docking to minimize distortions.
D. Four views of the human spoke show a striking similarity to the isolated yeast spoke. The three functional layers are labeled in the top view and the NE is visible in the side view.
E. A central cross-section of the algal NPC with a radially expanded inner ring (EMD-4355; (Mosalaganti et al., 2018)).
F. The algal spoke is similar to the *in situ* yeast spoke; however Nup170 β-propellers and local regions of the α-helical solenoid undergo a large movement and extended, α-helical coiled coils of the Nsp1 complex are more curved and may be more flexible. The 3D density map is consistent with the presence of two diagonal walls. Scale bars for similar panels (A/,C,/E) and (B,/D,/F) are indicated.

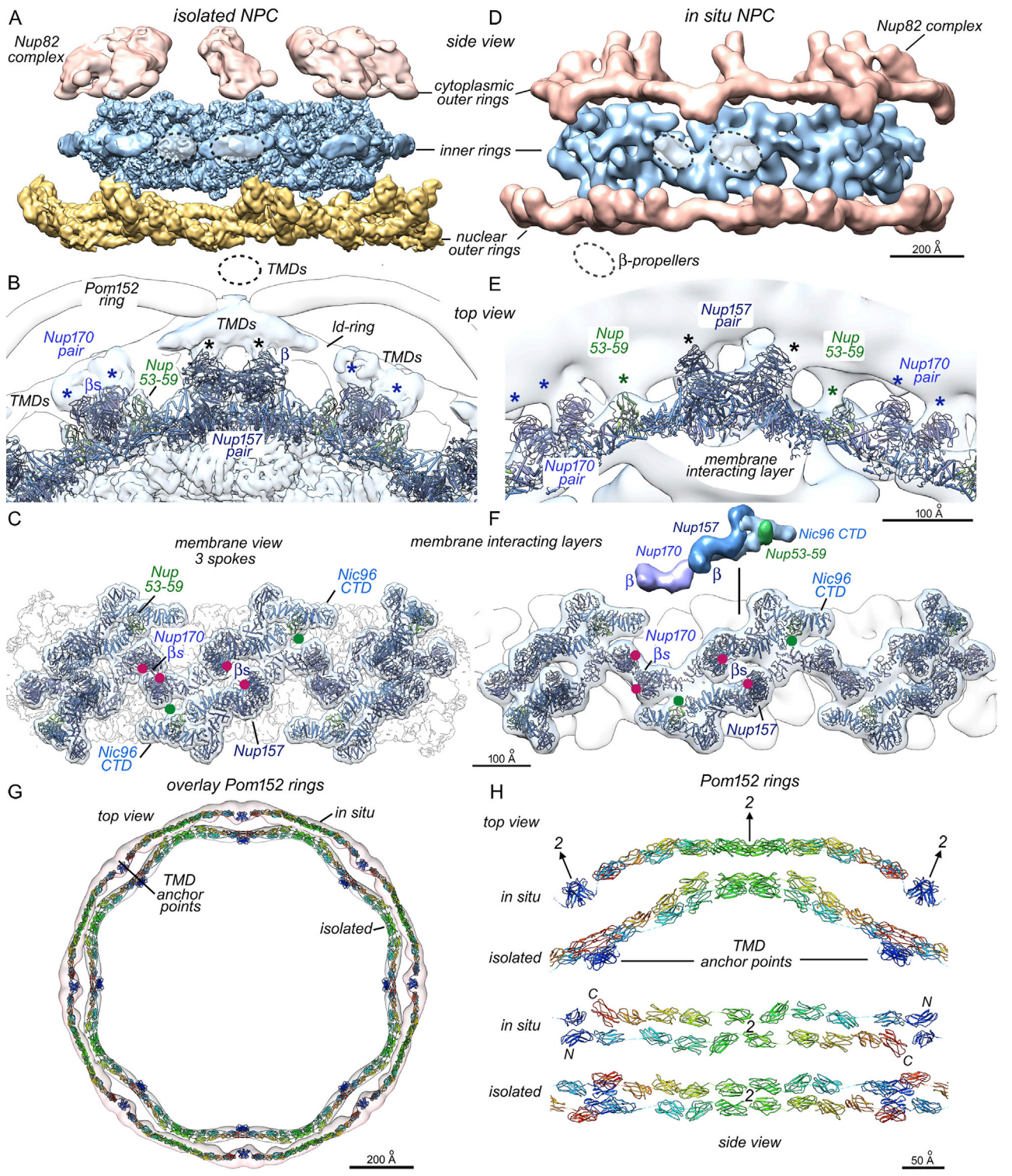

Figure S9. Membrane contacts of the inner ring and Pom152 rings, related to Figures 2 and 5

A. Membrane interactions of the isolated NPC. A side view from the NE lumen with contact sites to the lipid-detergent ring at local 2-fold axes are indicated (dashed ovals).

B. A view from the cytoplasm of the membrane interacting layer shows contact sites for Nup157 and Nup170 β-propellers (black and blue asterisks) with densities in the lipid-detergent ring (ld-ring) that may represent TMDs for Pom152/34 and Ndc1, respectively.

(legend continued on next page)

C. Membrane interacting layers from adjacent spokes form a nearly-continuous band when viewed from the pore membrane. Approximate positions of membrane anchor sites for β-propellers (red dots) and Nup53-Nup59 heterodimers (green dots) are indicated.

D. Membrane interactions of the *in situ* NPC. A dimeric clustering of β-propellers from Nup157 (center dashed oval) and Nup170 (left) is shown in a lumenal view without the pore membrane.

E. A view from the cytoplasm shows membrane interacting sites. The density distribution is asymmetric across the spoke 2-fold axis that passes between a pair of Nup157 molecules.

F. A side view is shown for the dilated inner ring with approximate positions of membrane anchor sites for β-propellers (red dots) and Nup53-Nup59 heterodimers (green dots). An icon view shows the relationship of the Nic96 CTD and Nup53-Nup59 with extended Nup157 and Nup170 molecules from the top half of one spoke.

G. Pom152 rings are overlaid to show changes in shape and diameter that occur during radial expansion. Rainbow colored models (N to C, blue to red) shown as "cylinders and strands" for isolated and *in situ* Pom152 rings docked in transparent density maps; spoke anchor points are indicated.

H. A 45 degree wedge from the aligned Pom152 rings is shown with their respective models. (**top**) The two Pom152 rings are viewed from the cytoplasm in rainbow colors; 2-fold axes and TMD anchors are labeled. (**bottom**) A lumenal view is shown in which two anti-parallel strands of Ig-like domains form a flat ribbon. Scale bars are indicated.